# Journal of Materials Chemistry A

Accepted Manuscript


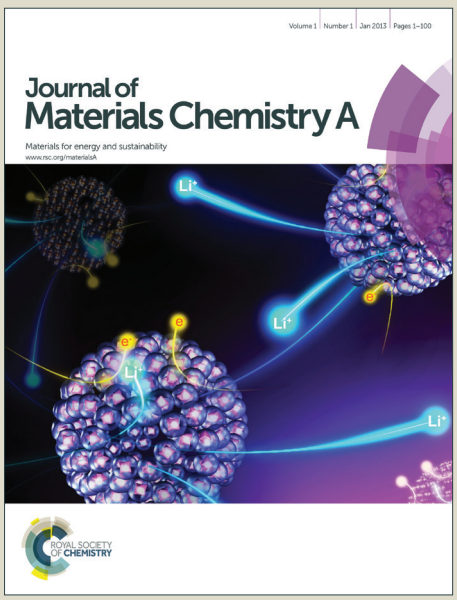





ROYAL SOCIETY OF CHEMISTRY

www.rsc.org/materialsA

Cite this: DOI: 10.1039/c0xx00000x

www.rsc.org/xxxxxx

ARTICLE TYPE

# Nickel-Substituted Zeolitic Imidazolate Frameworks for Time-Resolved Alcohol Sensing and Photo Catalysis under Visible Light

**Rui Li,[a] Xiaoqian Ren,[a] Hongwei Ma,[a] Xiao Feng,[a] Zhengguo Lin,[a] Xingguo Li,[b] Changwen Hu,*[a] and Bo Wang*[a]**

*Received (in XXX, XXX) Xth XXXXXXXXX 20XX, Accepted Xth XXXXXXXXX 20XX*
**DOI: 10.1039/b000000x**

**A facile strategy has been developed to introduce six-coordinated nickel clusters to zinc-based ZIF-8 structure via a one-pot mechanochmical synthesis under liquid assisted grinding (LAG) conditions. This Ni-substituted ZIF-8, denoted as BIT-11, can selectively pick different alcohol molecules according to their shapes and undergo a de-coordination to form stable four-coordinated Ni clusters denoted as BIT-11b. Alternatively single crystals of Ni-substituted ZIF-8 with similar coordination environment as BIT-11b are synthesized solvothermally. BIT-11b also shows exceptional photo-catalytic activity.**

The combination of dynamic activities with robustness in a synergetic manner is easily achieved down to molecular level in nature, yet remains a challenge in artificial materials.[1] For instance, nerve cells can sense and transmit subtle signals while enzyme molecules can effectively convert substrates to desirable compounds. In contrast, man-made chemical sensors and catalysts often lack the sensitivity and selectivity needed comparing to their biological counterparts. Furthermore architectural domain that work independently, yet are communicated, is common in biology but difficult to achieve in synthetic materials.

We believe that having different active yet interconnected domains in a well-defined open framework offers a useful strategy for achieving materials with higher complexity and functionalities.[2] Specifically the introduction of additional active and labile metal clusters into a robust metal-organic framework (MOF) structure can serve potential binding sites for selective sensing and catalysis.[3] However the use of MOFs so far has largely relied on nonspecific binding interactions to host small molecular guests.[4]

To introduce such active species into a MOF structure, one can apply solvothermal synthesis using mixed metal complexes as the starting material [5] or adopt the post-synthetic modification strategy to substitute the backbone metals with different metal clusters.[6] However in these reactions, thermally stable compounds will often form where the active and labile metal clusters are fully coordinated by the backbone ligands and consequently turned to inactive building units of the framework. Therefore, a mild yet simple approach is needed to retain the activity of the desirable metal clusters while forming the robust porous frameworks. Indeed our group had developed a new mechanical approach to encapsulate a Polyoxometallate (POM) cluster inside a MOF cage by ball milling.[7] And these "trapped" POM species maintained their activity as binding sites for drug molecules.

Herein we report a facile strategy to introduce meta-stable six-coordinated nickel clusters to zinc-based ZIF-8 structure via a one-pot mechanochmical method. Interestingly this Ni-substituted ZIF-8, denoted as BIT-11, can selectively pick different alcohol molecules according to their shapes and undergo a chemical-induced de-coordination to form stable four-coordinated Ni clusters denoted as BIT-11b (Fig. 1a). Similarly light purple crystals of a new Ni-substituted ZIF-8 structure with stable four-coordinated Ni centers, denoted as BIT-12, are also obtained by traditional solvothermal method (Fig. 1b, see Supporting Information Section 3 for details). Thus-obtained samples are fully characterized by single-crystal X-ray diffraction, powder X-ray diffraction (PXRD), index of the XRD patterns by Pawley fitting method, elemental analyses, FT-IR, TGA, diffuse reflectance visible spectra and gas adsorption measurements.

By virtue of the nano cages that are interconnected by the "revolving doors" in this meta-stable Ni-substituted BIT-11, such selective alcohol sensing triggered by coordination geometry change can be monitored by apparent absorption wavelength shift under visible light in a time-resolved manner. Since the visible color change of materials is one of the simplest yet most powerful ways to detect and signal guest molecules, this open framework with active metal centers can serve as a probe to explore guest-host interactions.[8] Furthermore such changes can also be observed in vapor phase and BIT-11b shows exceptional photo-catalytic activity.

BIT-11 was prepared via a one-pot mechanochemical method under liquid assisted grinding (LAG) at room temperature.[9] Zinc oxide (ZnO) and 2-methyl imidazole (HMeIM) with nickel acetate tetrahydrate ($Ni(OAc)_2 \cdot 4H_2O$) were put into the stainless steel milling pot, and ball-milled with trace amount of ethanol as the initiator using steel balls for 30 minutes. The solids were collected and green powders of BIT-11 were obtained. The Ni:Zn ratios can be adjusted by altering the initial relative amount of ZnO and $Ni(OAc)_2 \cdot 4H_2O$. Surprisingly, BIT-11 is very labile when exposed to alcohols. Specifically after soaking in MeOH, the color of BIT-11 immediately changed from green to violet

(Fig. 1a). In addition, we found that such violet BIT-11b can also be synthesized by stirring the mixtures of $Zn(NO_3)_2 \cdot 6H_2O$, $Ni(NO_3)_2 \cdot 6H_2O$, and HMeIM in methanol.

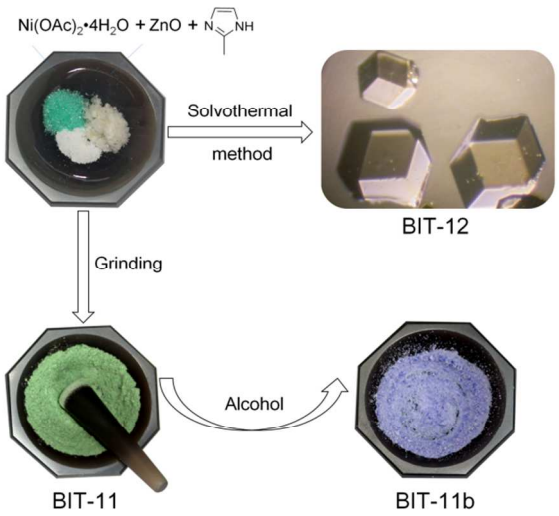


**Fig. 1** Schematic representation of the mechanochemical synthesis of BIT-11 and -11b, as well as the microscopic photo of BIT-12 single crystals synthesized solvothermally.

In the powder X-ray diffraction (PXRD) patterns, diffraction peaks of BIT-11 match well with those of pristine ZIF-8 with identical positions and relative intensities. Only a few extra peaks emerged (Fig. S2). The PXRD pattern of the violet sample BIT-11b was in good agreement with that of the ZIF-8. These results demonstrated that the two Ni-containing ZIF-8 frameworks, BIT-11 and -11b, adopted ZIF-8-like architectures with SOD topology. In order to identify the extra PXRD peaks in BIT-11, we milled ZIF-8 or HMeIM with $Ni(OAc)_2 \cdot 4H_2O$ under the same mechanochemical conditions as control experiments. The PXRD pattern of ZIF-8 milled with $Ni(OAc)_2 \cdot 4H_2O$ resembles that of ZIF-8, whereas the diffraction peaks of HMeIM milled with $Ni(OAc)_2 \cdot 4H_2O$ match well with the additional peaks in BIT-11. It shows that some crystalline Ni-HMeIM clusters that are produced by milling HMeIM with $Ni(OAc)_2 \cdot 4H_2O$ are formed and retained in the cavities of BIT-11.

The X-ray powder diffraction pattern of this Ni-HMeIM cluster was further indexed with $a$ = 26.1799 Å, $b$ = 7.7014 Å, $c$ = 7.5304 Å, $\alpha$ = 90°, $\beta$ = 90°, $\gamma$ = 90°, space group $P2_12_12_1$. Pawley fitting of the experimental data against above unit cell parameters converges with Rwp=3.74%, indicating that the calculated peak positions are in good agreement with the observed ones, and the sample is pure-phase. In this cluster Ni ions are surrounded by HMeIM and acetate (Fig. S3, see Supporting Information Section 4 for details). When we put the green Ni-HMeIM clusters into some polar solvents, i.e. MeOH, EtOH etc, it dissolves immediately and a transparent green solution is obtained. Since these green Ni-HMeIM clusters can be fully removed by washing with MeOH and no apparent color change is observed, it is reasonable to conclude that the color change from BIT-11 to BIT-11b is indeed caused by the coordination transformation of the backbone not the Ni-HMeIM clusters.

Moreover, SEM (Fig. S4) was also employed to confirm the microscopic architecture, which suggests that sample BIT-11b is indeed nanoparticles ranging from 50-200 nm. FT-IR spectrum of thus-obtained BIT-11b matches well with that of the ZIF-8 while the spectrum of the original BIT-11 differs from ZIF-8 (Fig. S5). The extra peaks in the FT-IR spectrum of BIT-11 are in good agreement with those of the sample prepared by milling HMeIM and $Ni(OAc)_2 \cdot 4H_2O$ and differ from $Ni(OAc)_2 \cdot 4H_2O$. This indicates no starting materials are trapped in the frameworks and only Ni-HMeIM clusters are present.

In consistence with PXRD results, the gas sorption measurements and elemental analyses further confirmed our findings. Based on the $N_2$ sorption isotherms at 77 K, the Brunauer-Emmett-Teller (BET) surface areas of BIT-11 with starting ZnO and $Ni(OAc)_2 \cdot 4H_2O$ ratios of 1:2, 1:1, and 2:1 were calculated to be 380, 660, and 950 $m^2/g$, respectively. In the meanwhile, the BET surface areas of BIT-11b (starting ratio ZnO: $Ni(OAc)_2 \cdot 4H_2O$ =1:2, 1:1, and 2:1) drastically increased to 1590 $m^2/g$, 1630 $m^2/g$, and 1490 $m^2/g$, which are slightly higher than that of mechanochemically prepared pristine ZIF-8 (1390 $m^2/g$) (Fig. 2a). The results also indicate that the cages in BIT-11 are indeed occupied by Ni-HMeIM clusters while all cages are empty in BIT-11b. Carbon dioxide ($CO_2$) adsorption isotherms of sample BIT-11 and BIT-11b collected at 273 K are proportional to $N_2$ adsorption isotherms (Fig. S9). In spite of the fact that Ni content in BIT-11 decreases upon removing the Ni-HMeIM clusters that are trapped in the cages, there are still Ni ions present in the framework of BIT-11b as evidenced by elemental analyses (Table S2) and XPS ((Fig. S7). Based on PXRD and gas sorption analyses, the residue Ni ions in the frameworks of both BIT-11 and -11b presumably substitute Zn(II) ions of the $[ZnN_4]$ clusters and are positioned in the backbones of the frameworks (Fig. S10). Controlled experiments show that the mixture of pristine ZIF-8 and Ni-HMeIM clusters turns from green to white after washing with MeOH and thus-obtained solid is confirmed as pure zinc-based ZIF-8 (as proved by PXRD, UV-vis and EA). Further the Ni-HMeIM clusters can be fully dissolved in MeOH or any other alcohols and the UV-vis absorption remains almost unchanged in both the solid and the solution (Fig. 2b). In contrast BIT-11 changes from green to violet (as BIT-11b) after thoroughly washing with MeOH (Fig. 2c). And the porosity of the BIT-11b is even higher than that of the pristine zinc-based ZIF-8.

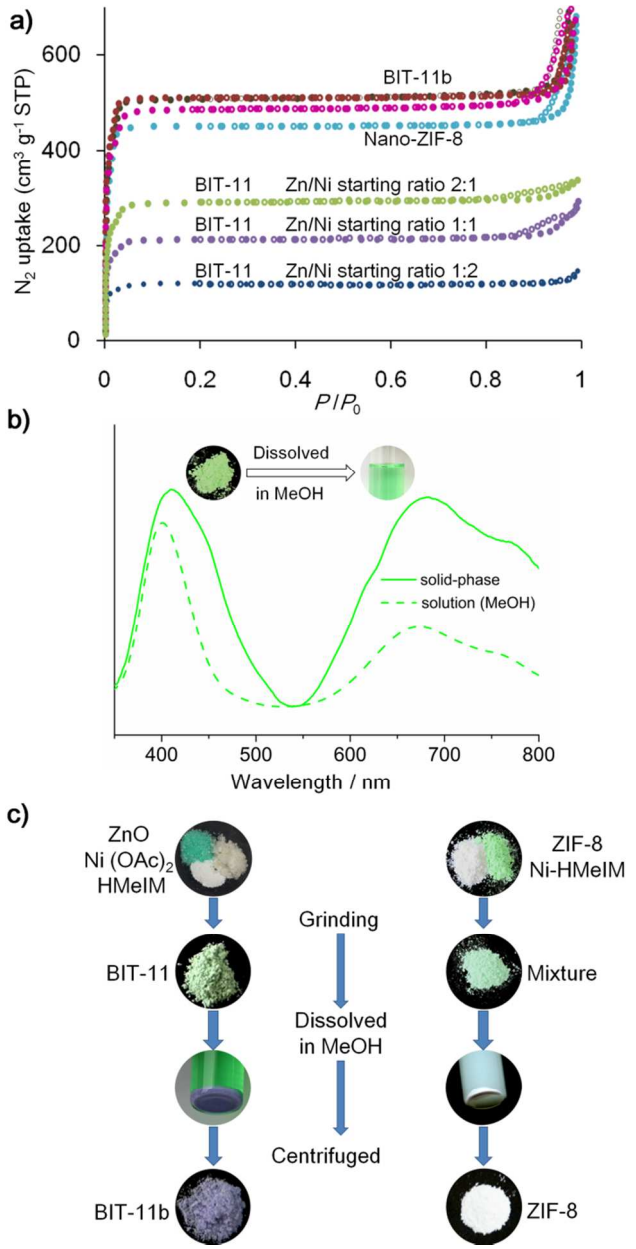


Fig. 2 (a) The $N_2$ adsorption isotherms of BIT-11 and -11b ( 77K ) obtained by various staring Zn/Ni ratio; isotherm of pristine ZIF-8 for comparison. (b) The UV-vis spectra of Ni-HmeIM clusters and the solution in MeOH. The inset photo highlights a transparent green solution of Ni-HMeIM in MeOH. (c) Schematic representation of BIT-11, and ball-milled ZIF-8 with Ni-HmeIM before and after dissolved in MeOH.

The diffuse reflectance visible spectra of BIT-11 and -11b are measured to evaluate the absorption features responsible for the color change from green to violet upon interaction with MeOH. The absorption peaks at 410 and 680 nm for BIT-11 (Fig. 3d) are originated from octahedral coordination of Ni(II) ions (Fig. 3b), which match well with those of six-coordinated tetrahydrate Ni(II) acetate and with those reported in the literature.[10] These band positions are characteristic of an octahedral coordination environment around a Ni(II) ion and are assigned as $^3A_{2g} \rightarrow {}^3T_{2g}$ and $^3A_{2g} \rightarrow {}^3T_{1g}$ (P) transitions.[11] In order to further prove that the Ni ions in backbones and cavities of BIT-11 are both six-coordinated, we checked the UV-vis spectrum of ball milled HMeIM with $Ni(OAc)_2 \cdot 4H_2O$ (Fig. S11). The existence of the characteristic peaks in the profile reveals that both backbone Ni ions and Ni-HMeIM clusters in the cavity are unambiguously octahedrally coordinated. However, these six-coordinated Ni ions are susceptible to MeOH due to their labile nature. This also reveals that the imidazole "revolving doors" on the cages of BIT-11 could help to stabilize the metastable six-coordinated Ni clusters. In the meantime, the absorption peaks at 580 and 790 nm for BIT-11b (Fig. 3e) are characteristic peaks of four-coordinated Ni ions (Fig. 3c) and can be attributed to the formation of violet color. The electronic absorption spectrum is assigned as the spin-allowed *d-d* transitions, $^3T_1$ (F) $\rightarrow {}^3A_2$(P) and $^3T_1 \rightarrow {}^1T_2$.[12]

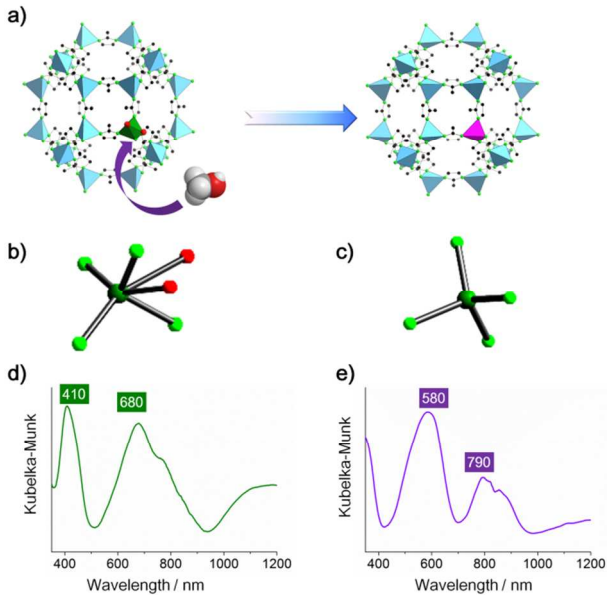


Fig. 3 (a) Schematic structure representation of the Ni coordination changes from preudo-octahedral to tetrahedral along upon exposing to methanol molecules. blue, light green, green, and black spheres represent Zn, Ni, N, and C atoms, respectively. Hydrogen atoms are omitted for clarity. (b) The coordination of the preudo-octahedral $[NiN_4O_2]$ unit. (c) The coordination of the tetrahedral $[NiN_4]$ unit. (e), (f) The diffuse reflectance UV-vis spectra of BIT-11 and -11b.

Fig. 3 shows that Ni(II) ions present in the backbones of BIT-11 are distorted six-coordinated with solvent molecules and four nitrogen atoms from imidazolate, where the chelating solvent molecules occupy part of the cages and partially block accessible cavities (i.e. BET 660 $m^2/g$ *vs*. 1630 $m^2/g$). Due to the size of the MeOH (2.438 Å by 1.818 Å comparing to 3.4 Å) of the framework aperture,[13] MeOH molecules can easily enter the cages of BIT-11, and not only cause the decomposition of the Ni-HMeIM clusters, but also force out the chelating solvent molecules on the backbone Ni ions. And consequently these MeOH molecules lead to the formation of stable $[NiN_4]$ clusters (Fig. 3a). The striking color change from green to violet was triggered by the coordination geometry change of Ni from preudo-octahedral to tetrahedral.

Dinc□ *et. al.* [5a, 5b] and others had reported MOFs with metal substitution can change color upon exposing to solvent molecules because these molecules can weakly coordinate to the metal

centers as in the case of any other MOFs with open metal sites (HKUST-1, MOF-74, MOF-14, etc.). However BIT-11 is the very first example where color change is triggered by decoordination process when the guest molecules attack the metastable metal centers buried inside the cages of MOFs.

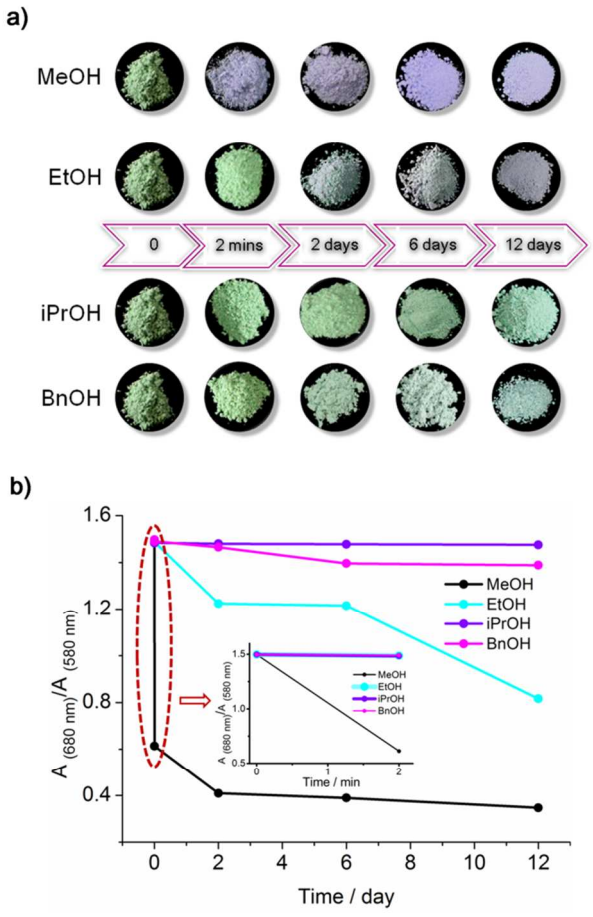


**Fig. 4** (a) The pictures of the apparent color changes for BIT-11 soaked in different alcohols at certain time intervals. (b) Absorption data of $A_{680}/A_{580}$ for BIT-11 upon soaking in variable alcohols over the time.

Based on the observed spectral changes, we selected BIT-11 as the chemical probe to selectively detect different guest solvent molecules. BIT-11 sample were immersed in methanol (MeOH), ethanol (EtOH), *i*-sopropanol (iPrOH), and benzyl alcohol (BnOH) respectively (Fig. S12). Then the solids were isolated by filtration and dried under vacuum after soaking for different periods of time. As shown in Fig. 4a, it only takes two minutes for BIT-11 soaked in MeOH to turn from green to violet. In contrast, it takes 12 days for BIT-11 soaked in EtOH to change to light purple. For the samples soaked in iPrOH and BnOH, the color remained almost unchanged irrespective of immersion time. The above visual observations can be qualitatively characterized by the diffuse reflectance UV-vis spectra (Fig. S13) and PXRD (Fig. S14, S15). We calculated the absorption data of $A_{680}/A_{580}$ for BIT-11 upon soaking in different alcohols over certain time periods and the results are shown in Fig. 4b and Table 1. It is clear that MeOH triggered a much greater response than any other solvents tested.

Table 1. Absorption data changes of $A_{680}/A_{580}$ for BIT-11 when immersed in different alcohols.

| solvent | 0 min | 2 min | 2 days | 6 days | 12 days |
|---|---|---|---|---|---|
| methanol | 1.497 | 0.613 | 0.409 | 0.389 | 0.347 |
| ethanol | 1.497 | 1.487 | 1.224 | 1.215 | 0.816 |
| isopropanol | 1.497 | 1.483 | 1.480 | 1.478 | 1.475 |
| benzyl alcohol | 1.497 | 1.490 | 1.465 | 1.396 | 1.389 |

Besides the liquid detection, such color change can even be triggered by MeOH vapor through simple evaporation process. The sample can turn into violet within one day under methanol vapor at ambient condition (Fig. S16). In comparison, BIT-11 sample will keep the original green color when exposed to other alcohol vapors. The solvatochromic and vapochromic responses confirmed the trend of the sensing selectivity of guest molecules with increasing steric bulkiness when approaching the labile six-coordinated Ni centers protected in the restrained cavities of the open frameworks. Only the alcohols with proper size and shape, such as MeOH, can easily diffuse into the cavities and attack the active binding sites without suffering severe steric hindrance (Fig. S17, Table S4).

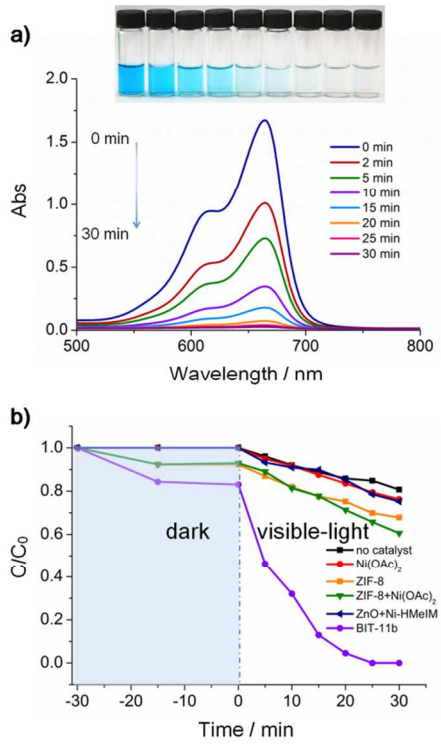


**Fig. 5** (a) UV−vis absorption spectra of MB solution degradation by BIT-11b under visible-light irradiation for different time intervals. The insert photograph highlights the experiment result of photodegradation, from left to right: MB solution, 0 min, 2 min, 5 min, 10 min, 15 min, 20 min, 25 min, 30 min. (b) Comparison of photocatalytic performance of MB degradation on samples under visible-light irradiation. ($C_0$=10 mg/L, 100 mL; the weight of catalyst = 20 mg).

Inspired by naturally occurred molecules, we believe that these active Ni(II) centers in the backbones of such highly selective open frameworks can also act as highly efficient catalyst. When we try to evaluate the photocatalytic activity of BIT-11 by photo-

degradation of methylene blue (MB) under visible-light irradiation in aqueous solution, BIT-11 immediately transformed into BIT-11b triggered by water molecules. Interestingly BIT-11b with relatively more stable four-coordinated Ni centers exhibits a remarkable photocatalytic activity (Fig. 5). The MB molecules disappeared within 25 min when BIT-11b is used as the photocatalyst, while isoreticular ZIF-8 structure without Ni components shows negligible activity (Fig. S18). The sample of BIT-11b remains unchanged as evidenced by the PXRD patterns before and after photo catalysis (Fig. S19). In addition, $Ni(OAc)_2$ also gives minimum catalytic activity. We suggest the mechanism is related to the excited electron from Ni which has variable valence. The electron is captured by electronegative substances such as molecular oxygen in solution, which would transform into highly active peroxide anion and subsequently accomplish further oxidation and degradation of MB. A similar mechanism has been proposed for the degradation of organic dyes in the presence of metal component.[14]

In summary, we developed a facile strategy to introduce active Ni metal centers into ZIFs via mechanochemical method under liquid assisted grinding (LAG) conditions. Both BIT-11 and -11b adopt ZIF-8 topology with Ni partially substituting the $ZnN_4$ in the backbone; nevertheless, the coordination modes of Ni in these two frameworks are distinct from each other. The Ni ions are distorted six-coordinated in BIT-11, whereas they are tetrahedrally coordinated in BIT-11b with enhanced stability. Meta-stable framework BIT-11 in green color can easily transform to violet BIT-11b triggered by small polar solvent molecules that can enter the narrow apertures of BIT-11 (i.e. MeOH, $H_2O$, EtOH etc.) and undergo a chemical-induced de-coordination. This transformation process can be utilized to selectively and precisely sensing and detecting different alcohol molecules in a time-resolved manner in both vapor and liquid phase. BIT-11b with photoactive Ni centers and open channels exhibits outstanding photocatalytic activity under visible light. The findings explored a simple yet powerful way to incorporate metal ions into the backbones of open framework materials without losing their activity. This may shed light on developing new complex metal-organic frameworks for energy and environmental applications as catalysis, photochemical and electrochemical materials.

## Notes and references

[a] *Key Laboratory of Cluster Science, Ministry of Education of China, School of Chemistry, Beijing Institute of Technology, 5 South Zhongguancun Street, Beijing, 100081, P.R. China.*
*E-mail: bowang@bit.edu.cn, cwhu@bit.edu.cn.*
[b] *College of Chemistry and Molecular Engineering, Peking University, 5 Yiheyuan Road, Beijing, 100871, P.R. China.*

† Electronic Supplementary Information (ESI) available: Synthetic materials and instruments, synthetic methods, X-ray crystal dada, experimental and simulated powder X-Ray diffraction patterns, SEM and FT-IR spectroscopy of samples, elemental analyses, the thermogravimetric analysis, gas adsorption analyses, the diffuse reflectance UV-vis spectroscopy of samples, solvatochromic and vapochromism effects experiments, and photodegradation of MB on samples under visible-light are included in the supporting information. See DOI: 10.1039/b000000x/

1 (a) M. Meilikhov, S. Furukawa, K. Hirai, R. A. Fischer and S. Kitagawa, *Angew. Chem. Int. Ed*. 2013, **52,** 341; (b) J. Du and R. K. O'Reilly, *Chem. Soc. Rev*. 2011, **40**, 2402.
2 (a) G. Lu, O. K. Farha, L. E. Kreno, P. M. Schoenecker, K. S. Walton, R. P. Van Duyne and J. T. Hupp, *Adv. Mater*. 2011, **23**, 4449; (b) B. Chen, Y. Yang, F. Zapata, G. Lin, G. Qian and E. B. Lobkovsky, *Adv. Mater.* 2007, **19**, 1693. (c) B. P. Biswal, D. B. Shinde, V. K. Pillai and R. Banerjee, *Nanoscale*, 2013, **5**,10556.
3 (a) B. Chen, L. Wang, F. Zapata, G. Qian and E. B. Lobkovsky, *J. Am. Chem. Soc*. 2008, **130**, 6718; (b) M. D. Allendorf, R. J. T. Houk, L. Andruszkiewicz, A. A. Talin, J. Pikarsky, A. Choudhury, K. A. Gall and P. J. Hesketh, *J. Am. Chem. Soc*. 2008, **130**, 14404; (c) B. Chen, L. Wang, Y. Xiao, F. R. Fronczek, M. Xue, Y. Cui and G. Qian, *Angew. Chem. Int. Ed*. 2009, **48**, 500; (d) B. V. Harbuzaru, A. Corma, F. Rey, J. L. Jordá, D. Ananias, L. D. Carlos and J. Rocha, *Angew. Chem. Int. Ed*. 2009, **48**, 6476.
4 (a) B. Wang, A. P. Côté, H. Furukawa, M. O. Keeffe and O. M. Yaghi, *Nature* 2008, **453**, 207; (b) J. R. Li, J. Sculley and H. C. Zhou, *Chem. Rev.* 2012, **112**, 869; (c) K. Sumida, D. L. Rogow, J. A. Mason, T. M. McDonald, E. D. Bloch, Z. R. Herm, T. Bae and J. R. Long, *Chem. Rev*. 2012, **112**, 724; (d) X. Kong, E. Scott, W. Ding, J. A. Mason, J. R. Long and J. A. Reimer, *J. Am. Chem. Soc*. 2012, **134**, 14341; (e) A. J. Graham, D. R. Allan, A. Muszkiewicz, C. A. Morrison and S. A. Moggach, *Angew. Chem. Int. Ed*. 2011, **50**, 11138. (f) Z. Zhang, W. Gao, L. Wojtas, S. Ma, M. Eddaoudi, and M. J. Zaworotko, *Angew. Chem. Int. Ed*. 2012, **51**, 9330; (g) Z. Zhang, L.Zhang, L. Wojtas, P. Nugent, M. Eddaoudi, and M. J. Zaworotko, *J. Am. Chem.Soc*. 2012, **134**, 924; (h) M. H. Alkordi, Y. Liu, R. W. Larsen, J. F. Eubank, and M. Eddaoudi, *J. Am. Chem.Soc***.** 2008, **130**, 12639.
5 (a) C. K. Brozek and M. Dinc□, *Chem. Sci*. 2012, **3**, 2110; (b) H. Li, W. Shi, K. Zhao, H. Li, Y. Bing and P. Cheng, *Inorg. Chem*. 2012, **51**, 9200; (c) J. A. Botas, G. Calleja, M. Sánchez-Sánchez and M. G. Orcajo, *Langmuir* 2010, **26**, 5300.
6 (a) M. Kim, J. F. Cahill, H. Fei, K. A. Prather and S. M. Cohen, *J. Am. Chem. Soc*. 2012, **134**, 18082; (b) S. Das, H. Kim and K. Kim, *J. Am. Chem. Soc*. 2009, **131**, 3814; (c) X. Song, T. K. Kim, H. Kim, D. Kim, S. Jeong, H. R.Moon and M. S. Lah, *Chem. Mater*. 2012, **24**, 3065; (d) Z. Zhang, L. Zhang, L. Wojtas, P. Nugent, M. Eddaoudi and M. J. Zaworotko, *J. Am. Chem.Soc*. 2012, **134**, 924; (e) J. Zhao, L. Mi, J. Hu, H. Hou and Y. Fan, *J. Am. Chem.Soc*. 2008, **130**, 15222; (f) T. Jacobs, R. Clowes, A. I. Cooper and M. J. Hardie, *Angew. Chem. Int. Ed*. 2012, **51**, 5192. (g) C. K. Brozek and M. Dinc□, *J. Am. Chem. Soc*. 2013, **135**, 12886;
7 R. Li, X. Ren, J. Zhao, X. Feng, X. Jiang, X. Fan, Z. Lin, X. Li, C. Hu and B. Wang, *J. Mater. Chem. A*, 2014, **2**, 2168..
8 (a) L. E. Kreno,. K. Leong, O. K. Farha, M. Allendorf, R. P. V. Duyne and J. T. Hupp, *Chem. Rev.* 2012, **112**, 1105; (b) G. Lu and J. T. Hupp, *J. Am. Chem.Soc*. 2010, **132**, 7832; (c) L. G. Beauvais, M. P. Shores and J. R. Long, *J. Am. Chem. Soc.* 2000, **122**, 2763; (d) Z. Lu, R. Zhang, Y. Li, Z. Guo and He. Zheng, *J. Am. Chem. Soc*. 2011, **133**, 4172; (e) O. S. Wenger, *Chem. Rev*. 2013, **113**, 3686.
9 (a) S. L. James, C. J. Adams, C. Bolm, D. Braga, P. Collier, T. Friščić, F. Grepioni, K. D. M. Harris, G. Hyett, W. Jones, A. Krebs, J. Mack, L. Maini, A. G. Orpen, I. P. Parkin, W. C. Shearouse, J. W. Steed and D. C. Waddell, *Chem. Soc. Rev.* 2012, **41**, 413; (b) P. J. Beldon, L. Fábián, R. S. Stein, A. Thirumurugan, A. K. Cheetham and T. Friščić, *Angew. Chem. Int. Ed.* 2010, **49**, 9640; (c) B. P. Biswal, S. Chandra, S. Kandambeth, B. Lukose, T. Heine, and R. Banerjee, *J. Am. Chem. Soc*. 2013, **135**, 5328; (d) S. Chandra, S. Kandambeth, B. P. Biswal, B. Lukose, S. M. Kunjir, M. Chaudhary, R. Babarao, T. Heine, and R. Banerjee, *J. Am. Chem. Soc*. 2013, **135**, 17853.
10 (a) M. L. Jacono, M. Schiavello and A. Cimino, *J Phys. Chem*. 1971, **75**, 1044. (b) B. S. Hammes and C. J. Carrano, *Inorg. Chem.* 1999, **38**, 3562.
11 N. Masciocchi, G. A. Ardizzoia, G. LaMonica, A. Maspero, S. Galli, and A. Sironi, *Inorg. Chem.* 2001, **40**, 6983.
12 (a) B. Zheng, M. O. Miranda, A. G. DiPasquale, J. A. Golen, A. L. Rheingold and L. H. Doerrer, *Inorg. Chem.* 2009, **48**, 4274; (b) D. M. L. Goodgame,. M. Goodgame and F. A. Cotton, *J. Am.*

*Chem.Soc*. 1961, **83**, 4161; (c) D.M. Gruen and R. L. McBeth, *J. Phys. Chem.* 1959, **63**, 393; (d) D. Forster and D. M. L. Goodgame, *J. Chem. Soc.* 1964, **85**, 2790; (e) H. A. Weakliem, *J. Chem. Phys*. 1962, **36**, 2117.

13 K. S. Park, Z. Ni, A. P. Côté, J. Y. Choi, R. Huang, F. J. Uribe-Romo, H. K. Chae, M. O. Keeffe and O. M. Yaghi, *Proc. Natl. Acad. Sci. USA* 2006, **103**, 10186.

14 (a) P. Mahata, G. Madras and S. Natarajan, *J. Phys. Chem. B* 2006, **110**, 13759; (b) Z. Yu, Z. Liao, Y. Jiang, G. Li and J. Chen, *Chem. Eur. J.* 2005, **11**, 2642.